This is the peer reviewd version of the followng article:

Multidimensional Trajectories Generation with Vibration Suppression Capabilities: the Role of Exponential B-splines / Moriello, L., Biagiotti, L., Melchiorri, C.. - 50:1(2017), pp. 6054-6059. (20th World Congress of the International-Federation-of-Automatic-Control (IFAC) Toulouse, FRANCE JUL 09-14, 2017) [10.1016/j.ifacol.2017.08.1374].

ELSEVIER SCIENCE BV
Terms of use:

The terms and conditions for the reuse of this version of the manuscript are specified in the publishing policy. For all terms of use and more information see the publisher's website.

16/10/2026 23:33

(Article begins on next page)

Multidimensional Trajectories Generation with Vibration Suppression Capabilities: the Role of Exponential B-splines ⋆

Lorenzo Moriello * **Luigi Biagiotti** ** **Claudio Melchiorri** *

* *Department of Electrical, Electronic and Information Engineering "Guglielmo Marconi", University of Bologna, Viale del Risorgimento 2, 40136 Bologna, Italy (e-mail: {lorenzo.moriello2},{claudio.melchiorri}@unibo.it).*
** *Department of Engineering "Enzo Ferrari", University of Modena and Reggio Emilia, via Pietro Vivarelli 10, 41125 Modena, Italy (e-mail: luigi.biagiotti@unimore.it).*

Abstract: In this paper, exponential B-spline trajectories are presented and discussed. They are generated by means of a chain of filters characterized by a truncated exponential impulse response. If properly tuned, the filters applied to a vibrating plant are able to cancel the oscillations and in this sense the resulting splines are optimized with respect to the problem of vibrations suppression. Different types of exponential B-spline are illustrated, with one or more exponential filters in the chain, and the procedure for the interpolation of a given set of desired via-points, with a proper choice of the control points, is shown. As a matter of fact, exponential B-splines, generated by means of dynamic filters, combine the vibration suppression capability of input shapers and smoothing filters with the possibility of exactly interpolating some via-points. The advantages of these curves are experimental proved by considering the motion of a spherical pendulum connected to the flange of an industrial robot.

Keywords: Vibration Suppression, Splines, Motion Control, Trajectory Planning, Input Shaper.

1. INTRODUCTION

In a number of industrial tasks a payload affected by vibrations and oscillations must be precisely positioned in space. Consider for instance the case of cranes used for heavy lifting and transportation in various industrial applications, that are affected by the swing of the payload, or robots with elastic elements, i.e. elastic joints or flexible links, whose performance is strongly influenced by the vibrations of the end-effector when the motion trajectories excite the vibratory modes. In these applications, where the oscillating dynamics is not easily detectable with the standard sensors that equip the plant and accordingly cannot be compensated by a feedback control action, the use of a feed-forward control is often the only option for reducing the vibrations. A common feed-forward technique called command shaping or input shaping [1], based on the convolution of the input signal with a train of impulses of proper amplitude and properly delayed in time, has been successfully used to cancel vibrations in a high-speed robotic workcell by T.Chang et al. (2003), in a flexible robot manipulator by Mohamed and Tokhi (2004), in different types of crane by Lewis et al. (1998); Singhose et al. (2006); Lawrence and Singhose (2010), in a robot for semiconductor wafer handling by Aribowo (2011), in a robot for liquid container transferring by Aribowo et al. (2015) and in many other industrial tasks. However, as highlighted by Singhose and Singer (1996), although very effective in vibration reduction, methods based on reference input shaping may be not useful for trajectory following applications in 3D space such as painting, cutting, etc. since they alter the commanded trajectory. Alternative methods to input shaping are based on so-called smoothers, that is filters that increase the smoothness, i.e. the number of continuous derivatives, of the reference signal, see Biagiotti and Melchiorri (2012); Xie et al. (2013); Biagiotti et al. (2015). Also in this case, if the smoother is applied to a given 3D trajectory it modifies the shape of the geometric path. However, it is worth noticing that by properly combining some of them in a cascade configuration, it is possible to generate B-spline trajectories which exactly cross the desired via-points and at the same time are able to suppress vibrations. This approach has been followed in Biagiotti and Melchiorri (2011), where polynomial B-spline trajectories have been obtained with a chain of average filters. In this paper, the results found in Biagiotti and Melchiorri (2011) are generalized by taking into consideration the so-called exponential B-spline trajectories, able to exactly suppress vibrations if their parameters (duration and exponential decay rate) are chosen on the basis of the dynamic characteristics of the oscillating plant. The experimental results performed on a spherical pendulum connected to the end-effector of a robot manipulator show the effectiveness of the proposed method.

⋆ This activity has been supported by the University of Modena and Reggio Emilia with the "FAR 2015" project.

[1] See Singer and Seering (1990) and Singh and Singhose (2002) among many others.

2. DYNAMIC FILTERS FOR EXPONENTIAL B-SPLINES GENERATION

The standard definition of a spline trajectory in the so-called B-spline form is

$$q(t) = \sum_{j=0}^{n-1} p_j \, B_j^d(t), \qquad t_0 \le t \le t_{n-1} \tag{1}$$

where $B_j^d(t)$, $j = 0, \ldots, n-1$, are the B-spline basis functions of order d defined for the knot vector $[t_0, t_1, \ldots, t_{n-1}]$ and p_j the control points which determine the shape of the curve. Note that the curve $q(t)$ does not cross the control points p_j, and in order to interpolate a given set of n via-points $q_i^\star$ it is necessary to compute p_j, $j = 0, \ldots, n-1$ by imposing interpolation conditions at the desired time-instants t_i, i.e.

$$q(t_i) = q_i^\star. \tag{2}$$

Once the control points have been fixed, the spline can be computed at any time instant $t \in [t_0, \, t_{n-1}]$ by calculating the basis functions $B_j^d(t)$ via numerical procedures usually based on recursion.

The use of uniform B-splines, i.e. B-splines characterized by an equally-spaced distribution of the knots $t_{j+1} - t_j = T$, $j = 0, \ldots n-2$, allows to greatly simplify the procedure for the curve calculation. As a matter of fact, in this case all the basis functions are identical besides a time translation

$$B_j^d(t) = B^d(t - jT), \qquad j = 0, \ldots, n-1$$

and accordingly

$$q_u(t) = \sum_{j=0}^{n-1} p_j \, B^d(t - jT), \qquad 0 \le t \le (n-1)T \tag{3}$$

Since a basis function of generic order d can be expressed as

$$\begin{aligned} B^d(t) &= \frac{1}{T} B^{d-1}(t) * B^0(t) \\ &= \underbrace{\frac{1}{T} B^0(t) * \frac{1}{T} B^0(t) * \ldots * \frac{1}{T} B^0(t)}_{d \text{ times}} * B^0(t), \end{aligned} \tag{4}$$

where $*$ denotes the convolution product and

$$B^0(t) = \begin{cases} 1, & \text{if } \; 0 \le t < T \\ 0, & \text{otherwise,} \end{cases} \tag{5}$$

the B-spline trajectory in (3) can be re-written in the form

$$q_u(t) = \underbrace{\frac{1}{T} B^0(t) * \ldots * \frac{1}{T} B^0(t)}_{d \text{ times}} * \sum_{j=0}^{n-1} p_j \, B^0(t - jT). \tag{6}$$

By Laplace transforming (6) it descends that the trajectory $q_u(t)$ can be generated by means of a chain of d dynamic fed by the staircase signal $p(t)$ obtained by maintaining the value of each control point p_j for the entire period $jT \le t < (j+1)T$. For more details see Biagiotti and Melchiorri (2010, 2012, 2013).

2.1 Uniform Exponential Spline

The definition of B-spline basis function in (4) and (5) leads to standard piecewise polynomial functions which are a linear combination of terms t^r, $r = 0, \ldots, d$. In

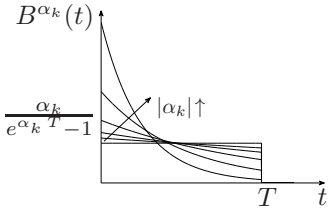

Fig. 1. Exponential basis-function $B^{\alpha_k}(t)$ for different values of parameter $\alpha_k < 0$.

Unser and Blu (2005) these polynomial B-splines have been generalized by assuming a different basis definition that allows to span the space of the functions composed by the elemental terms $t^r e^{\alpha_k t}$. Since the basic terms contain exponential functions the related curves are called exponential B-splines. In order to define such a kind of curve, it is necessary to consider a truncated exponential function in lieu of the rectangular function $B^0(t)$, i.e.

$$B^{\alpha_k}(t) = \begin{cases} \dfrac{\alpha_k T}{e^{\alpha_k T} - 1} e^{\alpha_k t}, & \text{if } \; 0 \le t < T \\ 0, & \text{otherwise,} \end{cases} \tag{7}$$

where α_k is a real parameter that defines the decay rate of the exponential function. In Fig. 1 the function $B^{\alpha_k}(t)$ is shown for different values of parameter $\alpha_k < 0$. Note that $\lim_{\alpha_k \to 0} B^{\alpha_k}(t) = B^0(t)$.

The (uniform) exponential basis function of order d is defined as

$$B^{(\alpha_0, \alpha_1, \ldots, \alpha_d)}(t) = \frac{1}{T} B^{\alpha_d}(t) * \ldots * \frac{1}{T} B^{\alpha_1}(t) * B^{\alpha_0}(t) \tag{8}$$

where parameters α_k can be freely chosen providing different types of B-spline curve. For instance

- $B^{(0,0,0,0)}(t) = B^3(t)$ leads to cubic polynomial trajectories;
- $B^{(0,0,0,\hat{\alpha})}(t)$ produces exponential splines of degree 3 that, in each knot span of duration T, are a linear combination of the functions 1, t, t^2, $e^{\hat{\alpha} t}$;
- $B^{(0,0,-\hat{\alpha},\hat{\alpha})}(t)$ produces the so-called exponential tension splines of degree 3, see Koch and Lyche (1993); Späth (1969), which are linear combination of the functions 1, t, $e^{-\hat{\alpha} t}$, $e^{\hat{\alpha} t}$;
- $B^{(\hat{\alpha}_0, \hat{\alpha}_1, \hat{\alpha}_2, \hat{\alpha}_3)}(t)$ produces B-splines that are a linear combination of the functions $e^{\hat{\alpha}_0 t}$, $e^{\hat{\alpha}_1 t}$, $e^{\hat{\alpha}_2 t}$, $e^{\hat{\alpha}_3 t}$.

For practical applications it is convenient that at least one of the parameters α_k is set to zero ($\alpha_0 = 0$). In this way exponential B-splines can be written as

$$q_e(t) = \underbrace{\frac{1}{T} B^{\alpha_d}(t) * \ldots * \frac{1}{T} B^{\alpha_1}(t)}_{d \text{ times}} * \sum_{j=0}^{n-1} p_j \, B^0(t - jT).$$

and the related B-spline filter for trajectory generator is a chain of the exponential filters

$$F_e^{\alpha_k}(s) = \frac{\alpha_k}{e^{\alpha_k T} - 1} \, \frac{1 - e^{\alpha_k T} \, e^{-T s}}{s - \alpha_k}, \tag{9}$$

fed by the staircase signal $p(t)$ defined for polynomial B-spline. Note that the basis function $B^{(\alpha_0, \alpha_1, \ldots, \alpha_d)}(t)$ is well defined even if some coefficients α_k are negative. In this case, the related filters $F_e^{\alpha_k}(s)$ are apparently unstable, being characterized by a positive real pole, but it is worth noticing that a cancellation between this pole and one the infinite zeros of the filter occurs. Moreover, since

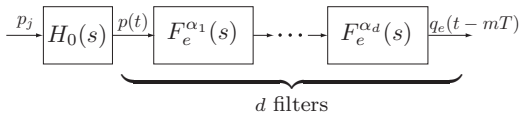

Fig. 2. System composed by d exponential filters and by a zero-order hold $H_0(s)$ for the computation of exponential B-spline trajectories of order d.

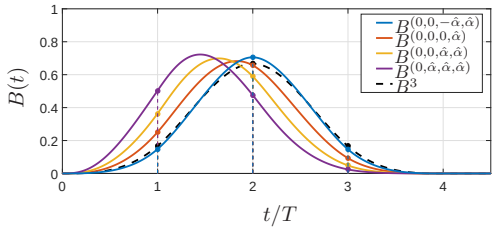

Fig. 3. Cubic B-spline basis function $B^3(t)$ and exponential B-spline basis function $B^{(\alpha_0,\alpha_1,\alpha_2,\alpha_3)}(t)$, for different configuration of the vector $(\alpha_0,\alpha_1,\alpha_2,\alpha_3)$. The numerical value $\hat{\alpha}=-2$ has been considered.

the filter has finite-length impulse response, its practical implementations in the discrete-time domain can be based on FIR filters which do not suffer from stability problems.

2.2 Control points calculation for interpolation

As already mentioned, in order to interpolate a given set of n via-points $q_i^\star$ the condition (2) must be imposed. For uniform B-splines the system of equations becomes

$$q_i^\star = q_e\Big((i-m)T\Big) = \sum_{j=0}^{n-1} p_j\, B^{(\alpha_0,\alpha_1,\ldots,\alpha_d)}\Big((i-j-m)T\Big), \quad (10)$$

where the additional delay $m\,T$, with $m=\frac{d+1}{2}$, has been added in order to make the system well conditioned from a numerical point of view. If a polynomial B-spline is considered, the basis function $B^d(t)$, which is shown in black in Fig. 3 for $d=3$ (cubic B-splines), is not null over the interval $]0,(d+1)T[$ and is symmetric with respect to the center $\frac{d+1}{2}T$, where the maximum of the function occurs. In this case, for a generic via-points the equation (10), that involves only a limited number of control points, is

$$\begin{aligned} q_i^\star = {} & p_{i-m+1}B_1^d \ldots + p_{i-1}B_{m-1}^d + p_i B_m^d + p_{i+1}B_{m+1}^d + \ldots \\ & + p_{i+m-1}B_{2m-1}^d, \end{aligned} \quad (11)$$

where B_k^d denotes $B^d(kT)$. By substituting the numerical values of the basis function and collecting all the equations, a linear system $\mathbf{Ap}=\mathbf{q}$ for the computation of the control points vector $\mathbf{p}$ is obtained, where $\mathbf{A}$ is a symmetric banded matrix. In case of cubic B-splines, whose basis function values are reported in Tab. 1, a tridiagonal system is obtained and in this case a solution can be found efficiently.

If exponential B-spline functions are considered, the control points can be computed with the same system of equations used for polynomial B-splines, i.e. (11), but substituting the values of the polynomial basis function $B^d(kT)$ with those of the exponential basis function $B^{(\alpha_0,\alpha_1,\ldots,\alpha_d)}(kT)$. Several cases are possible according to the different values of the vector $(\alpha_0,\alpha_1,\ldots,\alpha_d)$. In Fig. 3 the basis functions of exponential B-splines of degree 3 obtained with a unique parameter $\hat{\alpha}$ are shown, and the

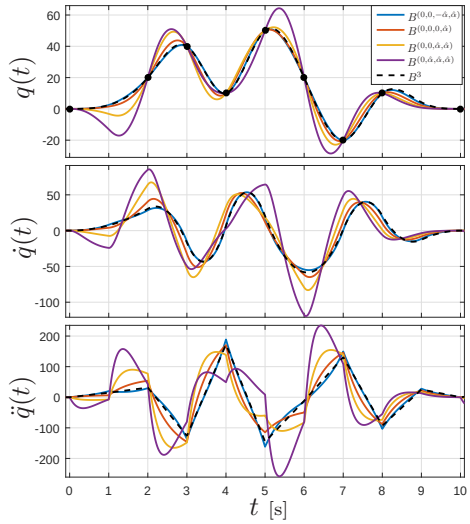

Fig. 4. Position, velocity and acceleration profiles of (scalar) uniform B-spline trajectories using the different basis functions of Fig. 3 with $T=1$ and $\hat{\alpha}=-1.7$.

related values at discrete time instants kT are reported in Tab. 1. Note that the symmetry of the functions, except for exponential spline under tension i.e. $B^{(0,0,-\hat{\alpha},\hat{\alpha})}(t)$, is lost especially for multiple exponential modes. This may lead to a system which is ill-conditioned from a numerical point of view, in particular when the parameter $\hat{\alpha}$ is quite large in magnitude.

In Fig. 4 the position, velocity and acceleration profiles of different types of exponential B-spline trajectories interpolating a set of given via-points are reported. Note that the peak values of velocity and acceleration tend to increase as the number of exponential filters in the B-spline generator augments.

3. VIBRATION SUPPRESSION WITH EXPONENTIAL B-SPLINES

Given an oscillating system, like for instance the controlled motion system composed by two masses with an elastic transmission considered in Biagiotti et al. (2015), whose dynamic model is

$$G_{ml}(s) = \frac{Q_l(s)}{Q_m(s)} = \frac{2\delta\omega_n s + \omega_n^2}{s^2 + 2\delta\omega_n s + \omega_n^2}, \quad (12)$$

where $Q_m(s)=\mathcal{L}\{q_m(t)\}$ and $Q_l(s)=\mathcal{L}\{q_l(t)\}$ are the Laplace transforms of the motor and load position, the typical feed-forward techniques for vibration suppression are based on input shaping Singhose (2009), system inversion Piazzi and Visioli (2000) or proper reference planning Kim and Agrawal (2006); Biagiotti and Melchiorri (2012); Béarée (2014). In particular, in Biagiotti et al. (2015) it has been shown that a dynamic filter like (9) placed before the input of the vibratory system (12) is able to completely suppress residual vibration for any reference signal provided that its parameters are chosen as

$$\alpha_k = -\delta\,\omega_n,\; T = k\,\frac{2\pi}{\omega_n\sqrt{1-\delta^2}},\; \text{being } k=1,2,\ldots. \quad (13)$$

The result, shown in Fig. 5(b) for a simple step input, can be explained by analyzing the poles and zeros of $F_e^{\alpha_k}(s)$ when the conditions (13) are met. In this case, it can be demonstrated that $F_e^{\alpha_k}(s)$ exactly cancel the poles of the

Table 1. Value of the B-spline basis function of degree 3 at discrete time instants kT.

	T	2T	3T
B^3	$\frac{1}{6}$	$\frac{4}{6}$	$\frac{1}{6}$
$B^{(0,0,0,\hat{\alpha})}$	$\frac{-2+2e^{\hat{\alpha}T}-(2+\hat{\alpha}T)\hat{\alpha}T}{2\hat{\alpha}^2T^2(-1+e^{\hat{\alpha}T})}$	$\frac{-4+\hat{\alpha}^2T^2+2\hat{\alpha}T\coth(\hat{\alpha}\frac{T}{2})}{2\hat{\alpha}^2T^2}$	$\frac{-2+e^{\hat{\alpha}T}(2+\hat{\alpha}T(-2+\hat{\alpha}T))}{2\hat{\alpha}^2T^2(-1+e^{\hat{\alpha}T})}$
$B^{(0,0,\hat{\alpha},\hat{\alpha})}$	$\frac{2+\hat{\alpha}T+(-2+\hat{\alpha}T)e^{\hat{\alpha}T}}{(\hat{\alpha}T)(-1+e^{\hat{\alpha}T})^2}$	$\frac{-(\hat{\alpha}T-\sinh(\hat{\alpha}T))\mathrm{csch}(\hat{\alpha}\frac{T}{2})^2}{\hat{\alpha}T}$	$\frac{e^{\hat{\alpha}T}(2+\hat{\alpha}T+(-2+\hat{\alpha}T)e^{\hat{\alpha}T})}{(\hat{\alpha}T)(-1+e^{\hat{\alpha}T})^2}$
$B^{(0,\hat{\alpha},\hat{\alpha},\hat{\alpha})}$	$\frac{-2+(2+(-2+\hat{\alpha}T)\hat{\alpha}T)e^{\hat{\alpha}T}}{2(-1+e^{\hat{\alpha}T})^3}$	$\frac{(-4+\hat{\alpha}^2T^2+2\hat{\alpha}T\coth(\hat{\alpha}\frac{T}{2}))\mathrm{csch}(\hat{\alpha}\frac{T}{2})^2}{8}$	$\frac{e^{2\hat{\alpha}T}(-\hat{\alpha}T(2+\hat{\alpha}T)+2(-1+e^{\hat{\alpha}T}))}{2(-1+e^{\hat{\alpha}T})^3}$
$B^{(0,0,-\hat{\alpha},\hat{\alpha})}$	$\frac{\mathrm{csch}(\hat{\alpha}\frac{T}{2})^2(-\hat{\alpha}T+\sinh(\hat{\alpha}T))}{4\hat{\alpha}T}$	$\frac{-\mathrm{csch}(\hat{\alpha}\frac{T}{2})^2(-\hat{\alpha}T\cosh(\hat{\alpha}T))+\sinh(\hat{\alpha}T))}{2\hat{\alpha}T}$	$\frac{\mathrm{csch}(\hat{\alpha}\frac{T}{2})^2(-\hat{\alpha}T+\sinh(\hat{\alpha}T))}{4\hat{\alpha}T}$

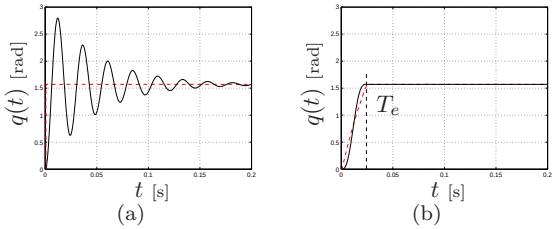

(a) (b)

Fig. 5. Response of a lightly damped vibratory system $G_{ml}(s)$ to a step input $q_{ref}(t)$ (a), compared to the response caused by the step filtered by $F_e^{\alpha_k}(s)$ (b). Reference trajectories are in red dashed line.

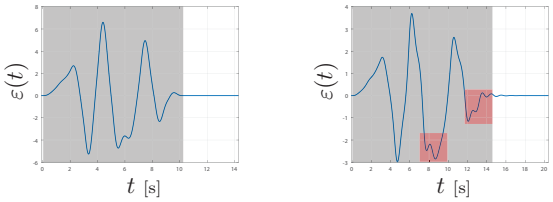

(a) (b)

Fig. 6. Responses of a second order system ($\delta = 0.2$, $\omega_n = 2\pi$) fed by exponential tension B-splines: in (a) nominal parameter are used while in (b) ω_n is assumed 30% lower than the nominal value. In red vibrations occurring during the motion are highlighted.

plant $G_{ml}(s)$, thus allowing a perfect compensation of the vibrating dynamics.

In conclusion, an exponential B-spline generator of order d, that incorporates at least 1 of such filters, automatically suppresses vibrations if the proper parameters are set. Note that the condition (13) limits the minimum duration of the spline trajectory, which cannot be freely chosen but depends on the system dynamics. For instance, a vibration-free B-spline trajectory through n via-points will require a total duration of $(n + \frac{d+1}{2})\frac{2\pi}{\omega_n\sqrt{1-\delta^2}}$ seconds.

The use of one filter in the chain it is sufficient to guarantee the vibration suppression property of the generated B-spline trajectory in nominal conditions, but the insertion of additional exponential filters characterized by the parameters (13) contributes to enhance the robustness with respect to modeling errors on δ and ω_n at the expense of a possible ill-conditioning of the linear system for the control points computation, especially for large value of δ, and higher velocity and acceleration peak values of the resulting trajectory, as highlighted in the previous section. In Fig. 6 the tracking error $\varepsilon(t)$ of an oscillating system to two different exponential tension B-splines is reported: in Fig. 6(a) the nominal parameters of the plant are used in the filters definition, while Fig. 6(b) shows the tracking error when an error of -30% on ω_n is made. Note that, although the trajectory in case (b) is slower than the nominal B-spline trajectory, the vibration suppression is no longer guaranteed.

A comparison between the tracking errors $\varepsilon(t)$ to exponential B-splines generated by means of different basis function is reported in Fig. 7. In particular residual vibrations are evaluated at the end of the motion and the robustness of the various methods is analyzed when the estimation of the parameter δ (Fig. 7(b)) or ω_n (Fig. 7(c)) is affected by a 10% error.

4. EXPERIMENTAL RESULTS

In order to evaluate the proposed method in 3D space, a spherical pendulum has been considered. It is composed by a spherical mass of 1 kg connected to the flange of an industrial manipulator by means of an inelastic string of 660 mm length and negligible weight, see Fig. 8(a). The motion system is a COMAU Smart5 Six industrial robotic arm, with a COMAU C4G Controller and a standard PC with an Intel Core 2 Duo 2.4 GHz processor and 1 GB of RAM. The COMAU Smart5 Six is a 6 DOF robot with anthropomorphic structure and a 6 kg payload. The robot is driven by the COMAU C4G Controller that performs both the position/velocity control (adaptive control) and the power stage management with current control of each joint. The C4G Controller also implements a software option called "C4G OPEN" that allows the integration of the robot control unit with the external personal computer, in order to develop complex control systems at high hierarchical level. The C4G Open architecture is based on a real time communication on Ethernet network between the controller and the real time PC. In particular the PC runs on the real-time operating system RTAI-Linux on a Ubuntu NATTY distribution with Linux kernel 2.6.38.8 and RTAI 3.9 that allows the trajectory generator to run with a sampling period $T_s = 2$ [ms].

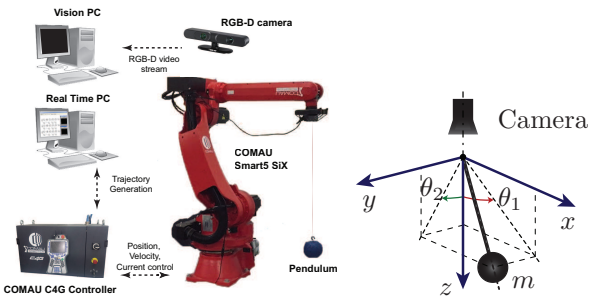

(a) (b)

Fig. 8. Experimental setup based on an industrial manipulator (a) and pendulum motion description in terms of angles θ_1 and θ_2 (b).

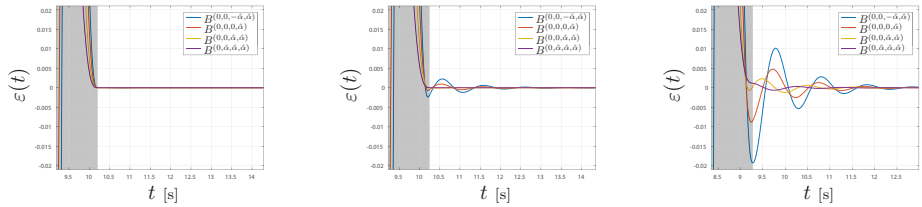

(a) (b) (c)

Fig. 7. Responses of a second order system ($\delta = 0.2$, $\omega_n = 2\pi$) to the trajectories of Fig. 4 (a) and responses of the same system assuming the presence of a 10% error in the estimation of parameter δ (b) and ω_n (c).

The robot flange is equipped with an ASUS Xtion PRO Live RGB-D camera, able to acquire both RGB and depth video streams at a frame rate of 30 fps, which allows to track the motion of the pendulum mass from the point of view of the pendulum pivot.

4.1 Pendulum model

The model of the spherical pendulum, linearized about its stable equilibrium point, can be written as two decoupled dynamics, i.e.

$$\ddot{\theta}_i + \delta\omega_n\theta_i + \omega_n^2\theta_i = \frac{u_i}{l}, \qquad i = 1, 2$$

where θ_1 and θ_2 denote the pendulum angle in the plane xz and yz respectively and u_1, u_2 are the accelerations imposed to the pendulum pivot along the coordinate axes x and y, see Fig. 8(b). The parameters δ and $\omega_n = \sqrt{g/l}$, where l is the length of the pendulum, are the same for both the dynamics. They can be precisely deduced with a simple identification procedure based on the observation of the free swing of the pendulum. The numerical values obtained with the experimental setup are

$$\omega_n^\star = 3.696 \text{ [rad/s]}\ , \quad \delta^\star = 2.306 \times 10^{-4}, \qquad (14)$$

that, inserted in (13), lead to the optimal (in terms of vibration suppression) exponential B-spline parameters

$$T = 1.7 \text{ [s]}\ , \quad \alpha = -8.523 \times 10^{-4}. \qquad (15)$$

Note that the value of ω_n is very similar to the theoretical one computed with $l = 660 + 50 = 710$ [mm], being the pendulum string of 660 [mm] length and the radius of the spherical mass 50 [mm], which results $\hat{\omega}_n = 3.71$ [rad/s].

4.2 3D task description

In order to properly evaluate the method, a typical pick and place trajectory has been planned. In particular the desired motion is composed of two straight segments joined with a circular arc as reported in black in Fig. 9. As well known this trajectory cannot be directly commanded to a robot since the junctions between lines and arcs produce acceleration discontinuities. As a consequence a cubic B-spline trajectory is used for approximating the motion in a smooth manner.

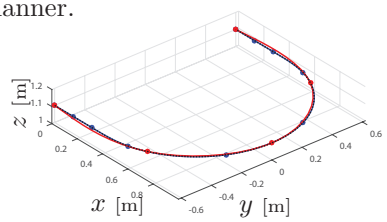

Fig. 9. Desired geometrical path (in black) and approximating B-splines: in blue is the standard B-spline, in red is the exponential tension B-spline. Via-points are reported with circles.

As a benchmark a standard B-spline $q(u)$ is computed at first by interpolating a set of via-points obtained by sampling the desired geometric path, and its motion law $u(t)$ is determined in order to minimize the acceleration along the curve. On the other hand an exponential tension B-spline interpolating the desired path through $n = 4$ via-points is considered. As already mentioned in Sec. 3 it has to be noted that the proposed method implies a constraint on the time duration of the motion. As a matter of fact, the uniform B-spline trajectory, whose knot span T is chosen accordingly to (13) in order to suppress the vibrations, has a total duration $T_{TOT} = (n + \frac{d+1}{2})T = 10.2$ seconds, being $d = 3$. Thus in order to perform a fair comparison the same duration T_{TOT} has been imposed to the feed-rate $u(t)$ of the standard B-spline.

Finally in lieu of a standard sampling, geometrically equidistant via-points have been chosen to be interpolated with the exponential tension B-spline. As a result the two spline trajectories approximate the desired path in different ways but completing the motion in the same time. In Fig. 10(b) the motion of the pendulum in terms of θ_1 and θ_2 when applying the standard B-spline trajectory and the exponential tension B-spline is shown. It can be noted that the pendulum swing is greatly reduced when the exponential tension B-spline is used. In particular the reduction is appreciable not only during the motion (in grey in Fig. 10(b)) where the sway can be influenced by inertial effects due to the acceleration of the robot, but especially when the motion ends where the residual pendulum oscillations are negligible with respect to the standard B-spline case.

This behavior is clearly illustrated in Fig. 11(a) and Fig. 11(b) where the position of the pendulum is reported with respect to the camera frame. In fact, the picture shows that, when the standard B-spline is adopted, the

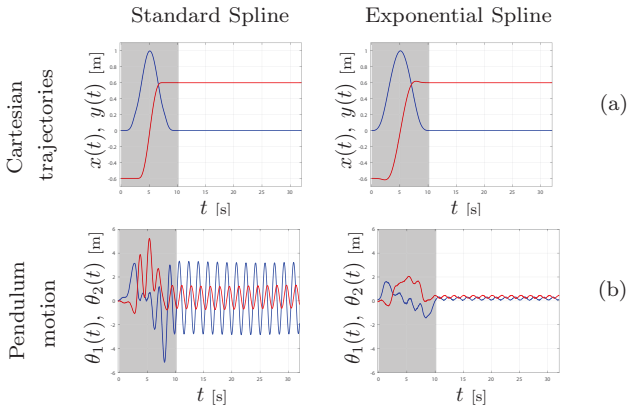

Fig. 10. B-spline trajectories in cartesian coordinates (a) and respective pendulum motion (b).

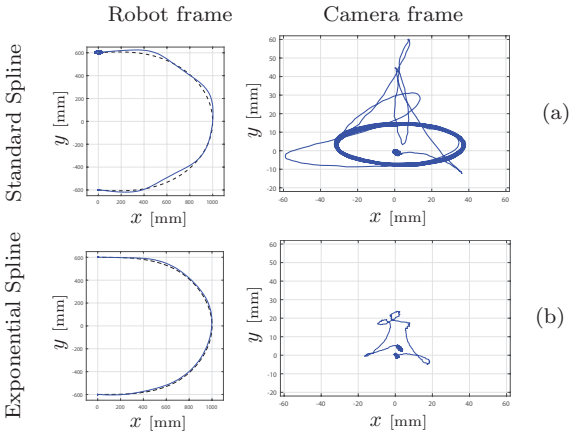

Fig. 11. Pendulum motion when applying the standard B-spline trajectory (a) and the exponential B-spline (b).

pendulum mass undergoes large swings and describes elliptical oscillations after the motion has ended. The adoption of exponential tension B-splines instead greatly reduces the swings during the motion and nearly suppresses oscillations at the end.

5. CONCLUSION

In this paper B-spline trajectories are optimized with respect to the problem of vibrations suppression. In this way, given a desired task in 3D space a vibration free trajectory can be directly generated by means of a chain of dynamic filters, preserving the geometrical path which is defined accordingly to the via-points, without the need of additional filtering processes that alter the commanded trajectory.

Vibration suppression ability of different exponential B-spline trajectories defined by means of different basis functions are evaluated and compared in terms of robustness with respect to errors in parameters, showing that:

- at least one exponential function $B^{\alpha_k}(t)$ is required in the basis function definition for vibration suppression;
- robustness is augmented as the number of exponential function $B^{\alpha_k}(t)$ involved in the basis function definition increases;
- the symmetry of the basis functions, except for exponential tension B-spline i.e. $B^{(0,0,-\hat{\alpha},\hat{\alpha})}(t)$, is lost especially for multiple exponential modes. This may lead to an ill-conditioned system for the control points calculation.

Finally the proposed approach, based on the exponential tension B-spline trajectory, is implemented to command an industrial manipulator supporting a spherical pendulum. The resulting motion of the pendulum demonstrates the effectiveness of the method especially if compared to the pendulum motion caused by a standard B-spline curve.

REFERENCES

Aribowo, W., Yamashita, T., and Terashima, K. (2015). Integrated trajectory planning and sloshing suppression for three-dimensional motion of liquid container transfer robot arm. *J. of Robotics*, 2015.

Aribowo, W.e.a. (2011). Vibration control of semiconductor wafer transfer robot by building an integrated tool of parameter identification and input shaping. *18th IFAC World Congress*, 44(1).

Béarée, R. (2014). New damped-jerk trajectory for vibration reduction. *Control Engineering Practice*, 28(0).

Biagiotti, L. and Melchiorri, C. (2011). Input shaping via b-spline filters for 3-d trajectory planning. In *IEEE/RSJ Int. Conf. on Intelligent Robots and Systems*.

Biagiotti, L., Melchiorri, C., and Moriello, L. (2015). Optimal trajectories for vibration reduction based on exponential filters. *IEEE Trans. on Control Systems Technology*, (99).

Biagiotti, L. and Melchiorri, C. (2010). B-spline based filters for multi-point trajectories planning. In *IEEE Int. Conf. on Robotics and Automation*.

Biagiotti, L. and Melchiorri, C. (2012). FIR filters for online trajectory planning with time- and frequency-domain specifications. *Control Engineering Practice*, 20.

Biagiotti, L. and Melchiorri, C. (2013). Online trajectory planning and filtering for robotic applications via b-spline smoothing filters. In *IEEE/RSJ Int. Conf. on Intelligent Robots and Systems*.

Kim, J.J. and Agrawal, B. (2006). Experiments on jerk-limited slew maneuvers of a flexible spacecraft. In *AIAA Guidance, Navigation, and Control Conferences*.

Koch, P.E. and Lyche, T. (1993). Geometric modelling. chapter Interpolation with Exponential B-splines in Tension, 173–190. Springer-Verlag, London, UK.

Lawrence, J. and Singhose, W. (2010). Command shaping slewing motions for tower cranes. *J. Vib. Acoust.*, 132(1).

Lewis, D., Parker, G.G., Driessen, B., and Robinett, R.D. (1998). Command shaping control of an operator-in-the-loop boom crane. In *Proc. of the American Control Conference*, volume 5.

Mohamed, Z. and Tokhi, M. (2004). Command shaping techniques for vibration control of a flexible robot manipulator. *Mechatronics*, 14(1).

Piazzi, A. and Visioli, A. (2000). Minimum-time system-inversion-based motion planning for residual vibration reduction. *IEEE/ASME Trans. on Mechatronics*, 5(1).

Singer, N.C. and Seering, W.P. (1990). Preshaping command inputs to reduce system vibration. *ASME J. of Dynamic Systems, Measurement, and Control*, 112.

Singh, T. and Singhose, W. (2002). Tutorial on input shaping/time delay control of maneuvering flexible structures. In *Proc. of the American Control Conference*.

Singhose, W., Lawrence, J., Sorensen, K., and Kim, D. (2006). Applications and educational use of crane oscillation control. *FME Trans.*, 34(4).

Singhose, W. (2009). Command shaping for flexible systems: A review of the first 50 years. *Int. J. of Precision Engineering and Manufacturing*, 10(4).

Singhose, W.E. and Singer, N.C. (1996). Effects of input shaping on two-dimensional trajectory following. *IEEE Trans. on Robotics and Automation*, 12(6).

Späth, H. (1969). Exponential spline interpolation. *Computing*, 4.

T.Chang, K.Godbole, and E.Hou (2003). Optimal input shaper design for high-speed robotic workcells. *J. Vib. Control*, 9(12).

Unser, M. and Blu, T. (2005). Cardinal exponential splines: part i - theory and filtering algorithms. *IEEE Trans. on Signal Processing*, 53(4).

Xie, X., Huang, J., and Liang, Z. (2013). Vibration reduction for flexible systems by command smoothing. *Mechanical Systems and Signal Processing*, 39(1–2).